

## Physicochemical Properties and Characterisation of Activated Carbon Prepared From Palm Kernel Shell

Suleiman Idris\*, Yunusa Muhammad Boyi, Wasiu. Jamiu, Nura Kontagora and Precious Adepeju Job

Received: 22 November 2025/Accepted: 26 March 2026 /Published: 20 April 2026

<https://dx.doi.org/10.4314/cps.v13i4.6>

**Abstract:** Palm kernel shells, which are free and naturally abundant, were employed for activated carbon preparation using  $H_3PO_4$  and  $ZnCl_2$  activating agents. Research findings indicated AC1 with an ash content of  $8.23 \pm 0.11\%$ , and that of AC2 was  $7.03 \pm 0.01\%$ , moisture content for AC1 and AC2 was  $7.61 \pm 0.02\%$  and  $7.05 \pm 0.04\%$  indicating a well-dried and packaged activated carbon. The results also indicated  $15.04 \pm 0.15\%$  for AC1 and  $14.87 \pm 0.05\%$  for AC2, with good fixed carbon content of  $69.12 \pm 0.01\%$  for AC1 and  $71.05 \pm 0.04\%$  for AC2 since the value for the fixed carbon content should be equal to or greater than 65% for a good activated carbon. The BET surface area of  $976.48 \text{ m}^2/\text{g}$  recorded for AC2 was high compared to  $815.38 \text{ m}^2/\text{g}$  indicated for AC1, and total pore volume of  $0.30 \text{ cm}^3/\text{g}$  and  $0.46 \text{ cm}^3/\text{g}$  was revealed for AC1 and AC2, respectively. The prepared activated carbons are both mesopores that are crucial in facilitating the access of the adsorbate molecules to the interior of the carbon particles. FTIR spectrum for AC1 indicated the peak occurrence at  $1735.1 \text{ cm}^{-1}$  and this may be attributed to the  $C = O$  stretching vibration. The presence of the absorption band at  $1996.0 \text{ cm}^{-1}$  is responsible for the presence of the  $C = C = C$  stretching vibration. The peak around  $2109.7$  and  $2883.1 \text{ cm}^{-1}$  could also be attributed to  $C \equiv C$  and  $C-H$  stretching bond. Also, for the AC2 spectral, the presence of the peak at  $875.9 \text{ cm}^{-1}$  indicates  $C = C$  stretching vibration, while the peak at  $1032.5 \text{ cm}^{-1}$  reveals  $C-O$  stretching, and the peak at  $2883.1 \text{ cm}^{-1}$  shows  $C-H$  stretching bond respectively.

**Keywords:** Functional Group, Pore Diameter, Mesopore, Surface Area, Porosity

**Suleiman Idris\***

Department of Chemistry, Federal University of Technology, Minna, Niger State, Nigeria

Email: [suleimandidris@futminna.edu.ng](mailto:suleimandidris@futminna.edu.ng)

<https://orcid.org/0009-0007-9559-556X>

**Yunusa Muhammad Boyi**

Department of Chemistry, Shehu Shagari University of Education, Sokoto, Sokoto State, Nigeria

Email: [yunus.boyi@yahoo.com](mailto:yunus.boyi@yahoo.com)

<https://orcid.org/0009-0005-4059-2965>

**Wasiu. Jamiu**

Department of Science Laboratory Technology, Chemistry Unit, Kwara State Polytechnic, Ilorin, Nigeria

Email:

[jamiu.wasiu@kwarastatepolytechnic.edu.ng](mailto:jamiu.wasiu@kwarastatepolytechnic.edu.ng)

<https://orcid.org/0000-0003-1610-5395>

**Nura Kontagora**

Department of Physical Sciences, Niger State Polytechnic, Zungeru, Niger State, Nigeria

Email: [nurakontagora090@gmail.com](mailto:nurakontagora090@gmail.com)

<https://orcid.org/0009-0007-5872-7877>

**Precious Adepeju Job**

Department of Chemistry, Federal University of Technology, Minna, Niger State, Nigeria

Email: [jobprecious43@gmail.com](mailto:jobprecious43@gmail.com)

<https://orcid.org/0009-0006-2323-5920>

### 1.0 Introduction

Activated carbon is a highly versatile porous carbonaceous material widely used for its exceptionally large surface area, well-developed pore structure, and diverse surface functional groups. These intrinsic properties, including micro- and mesoporous structures

and abundant surface functionalities, make activated carbon highly effective in adsorption, catalysis, and electrochemical applications (Danish & Ahmad, 2018). Activated carbon has a very broad range of applications across different industries, such as gas separation and storage, water treatment, industrial purification, catalysts and catalyst supports, supercapacitors, and electrodes. Traditionally, activated carbon is produced from non-renewable precursors such as coal; however, due to environmental concerns and the depletion of fossil resources, increasing attention has shifted toward renewable biomass-derived precursors (Wang *et al.*, 2013; Abioye & Ani, 2015; Karthikeyan *et al.*, 2018; Jalalah *et al.*, 2021). Chemical activation using agents such as phosphoric acid ( $H_3PO_4$ ) and zinc chloride ( $ZnCl_2$ ) has been widely reported to enhance pore development, surface area, and functional group distribution, although their comparative effects on specific biomass precursors remain insufficiently explored. In addition, the utilization of waste biomass for the production of activated carbon contributes to decreasing the costs of waste disposal and the negative impact on the environment. Numerous studies have investigated the conversion of various biomass wastes into activated carbon with promising adsorption performance and structural properties. These include wood and woody materials such as *Eucalyptus*, *jatropha*, and *E* fruit shells and hulls. Some of the fruit hulls used for the preparation of activated carbon are jatropha hulls, oat hulls, peanut hulls, rice hulls, and corn hulls. For good development of surface, structural and textural characteristics, biomass with high fixed carbon content and low ash content are desirable (Tongpoothorn *et al.*, 2011; Xin-Hui *et al.*, 2011; Yorgun & Yıldız, 2015).

Despite extensive research on biomass-derived activated carbon, there remains a lack of detailed comparative studies on the influence

of different chemical activating agents on the physicochemical and surface properties of palm kernel shell-derived carbon. In particular, limited information is available on how activating agents such as  $H_3PO_4$  and  $ZnCl_2$  affect pore structure development, surface chemistry, and adsorption potential. Addressing this gap is essential for optimizing the performance of activated carbon derived from locally available agricultural wastes.

This study aims to synthesize and characterize activated carbon derived from palm kernel shell using phosphoric acid ( $H_3PO_4$ ) and zinc chloride ( $ZnCl_2$ ) as chemical activating agents. The physicochemical properties, including surface area, pore size distribution, pore volume, and pore diameter, were evaluated using Brunauer–Emmett–Teller (BET) analysis, while Fourier Transform Infrared (FTIR) spectroscopy was employed to identify surface functional groups. The outcomes of this study are expected to provide valuable insights into the optimization of low-cost, sustainable activated carbon for environmental and industrial applications, particularly in adsorption-based water treatment systems.

## 2.0 Materials and Methods

### 2.1 Sample Collection and Preparation

Palm kernel shells were collected from the surroundings of a vegetable oil processing area. The palm kernel shells were cleaned of any visible dirt, debris, or leftover nut fragments. They were ground into powdered form and stored for further use.

### 2.2 Preparation of Activated Carbon

#### 2.2.1 Carbonisation

5 g of powdered palm kernel shells was weighed into clean crucibles.

The crucibles were placed in a muffle furnace at 800 °C for 15 minutes. The hot samples were then quenched in cold water for rapid cooling, washed thoroughly three times with distilled water, and dried in an oven at 100 °C for 1 hour. This process was repeated until a sufficient



quantity of carbonized sample was obtained (Fan *et al.*, 2005; Rahman *et al.*, 2005 & Idris *et al.*, 2013).

### 2.2.2 Activation Process

5 g of carbonized sample was impregnated separately with 5 cm<sup>3</sup> of 1 M H<sub>3</sub>PO<sub>4</sub> and 1 M ZnCl<sub>2</sub> solutions. The mixtures were allowed to stand for 24 hours, after which they were washed with tap water followed by distilled water until neutral pH (≈7) was achieved then excess water was removed and sample dried in the oven at 100<sup>0</sup>C for one hour and the activated carbon stored in air tight container for further use (Fan *et al.*, 2005; Rahman *et al.*, 2005; Idris *et al.*, 2013). Two activated carbons were produced, namely AC1 (H<sub>3</sub>PO<sub>4</sub>-activated carbon) and AC2 (ZnCl<sub>2</sub>-activated carbon).

## 2.3 Determination of Physicochemical Properties of the Activated Carbon

### 2.3.1 Volatile matter

Volatile matter content was determined according to the standard method (ASTM: D 2974-2014, Boadu *et al.*, 2018; Onawumi *et al.*, 2021). 1g of activated carbon was measured into a pre-dry crucible and covered with a lid, then heated in a Gallenkamp muffle furnace regulated at 950<sup>0</sup>C for 30 minutes. After heating, the plate was cooled in desiccators and weighed. The amount weighed was taken as volatile matter.

### 2.3.2 Determination of moisture content

2g of the activated carbon was weighed into a crucible. The sample was dried in the oven at a temperature of 1000 °C for 3 hours, cooled in a desiccator and weighed. The drying and weighing were repeated twice until a constant weight was obtained and recorded (ASTM: D 2974-2014, Boadu *et al.*, 2018 ; Onawumi *et al.*, 2021).

$$\%moisture = \frac{w_i - w_f}{w_i} \times \frac{100}{1} \quad (1)$$

where w<sub>i</sub>= Initial weight of activated carbon and w<sub>f</sub>= Final weight after drying

### 2.3.3 Determination of Ash Content

A clean and dry crucible was weighed (W<sub>0</sub>) and 1 gram of the powdered sample was added to the crucible, and the combined weight of the crucible and sample was recorded (W<sub>1</sub>). The crucible was placed in a muffle furnace set to 650<sup>0</sup>C and heated for 3 hours until a greyish-white ash was obtained. After this period, the crucible was removed and allowed to cool to room temperature before weighing. The weight of the residue after ashing was recorded as (W<sub>2</sub>) (Fan *et al.*, 2005; Rahman *et al.*, 2005; Idris *et al.*, 2013).

$$\% Ash = \frac{w_2 - w_0}{w_1 - w_0} \times \frac{100}{1} \quad (2)$$

where w<sub>0</sub>= weight of crucible, w<sub>1</sub>= weight of crucible + activated carbon, w<sub>2</sub>= weight of crucible + ashed activated carbon.

### 2.3.4 Determination of fixed carbon

The fixed carbon(FC) was determined as follows.

$$FC(\%) = 100 - (MC + AC + VM)\% \quad (3)$$

where MC is the moisture content, AS is the ash content, and VM is the volatile matter/

### 2.3.5 Bulk Density of Activated Carbon

A 25 cm<sup>3</sup> cylinder was filled to a given volume with activated carbon. The cylinder was tapped for at least 1 minute to compress the carbon to a steady volume. The compressed sample was weighed, and the mass (M) was divided by the volume occupied in the cylinder (V).

$$\text{Bulk density(g/cm}^3\text{)} = \frac{\text{Mass}}{\text{Volume}} \quad (4)$$

### 2.3.6 pH and Conductivity Measurement

According to the method described by Okieimen *et al.* (2004), 1.0 g of activated carbon was weighed into a beaker, and 20 cm<sup>3</sup> of distilled water was added. The sample was macerated with a long glass rod to ensure uniform wetting. The water volume was increased to 100 cm<sup>3</sup>. The sample was then stirred for 30 seconds and left to stand for 1 hour. Throughout the experiment, the beaker was covered with clean, washed glass covers. After the standing period, 10 cm<sup>3</sup> of the extract was decanted into a clean, dry beaker. The pH and conductivity of the extract was measured



immediately using a pH meter and a conductivity meter at room temperature.

### 2.3.7 Yield of Activated Carbon

The yield of activated carbon is defined as the ratio of the weight of the resultant activated carbon to the weight of the original precursor, measured on a dry basis (Yulu *et al.*, 2001).

$$\% \text{Yield} = \frac{\text{weight of AC}}{\text{weight of precursor}} \times \frac{100}{1} \quad (5)$$

## 2.4 Characterisation of Activated Carbon

### 2.4.1 Brunauer-Emmett-Teller (BET)

The Brunauer-Emmett-Teller (BET) Surface was determined by nitrogen adsorption at 77 K. The nitrogen gas adsorption measurements were done after the carbon was degassed at 300 °C in an inert condition for 24 hours. The BET surface area, mesopore volume, micropore surface area and pore diameter of the activated carbon were determined by the application of the Brunauer- Emmett-Teller (BET), Dubinin-Asthakov (DA) and BJH (Barrett–Joyner–Halenda) analysis software, respectively (Munagapati & Dong-Su, 2016; Boadu *et al.*, 2018).

### 2.4.2 Fourier Transform Infrared Spectrometer

(Themo Nicolet, model magna 760) was used to determine the functional groups of the activated carbon using the pellet press disk technique. The adsorbent/KBr mass ratio was 100:1. The spectral scanned at the rate of 10 nms<sup>-1</sup> ranged from 4000 to 400 cm<sup>-1</sup>.

## 3.0 Results and Discussion

### 3.1 Physicochemical Properties of the Activated Carbon

The results showed that AC1 had an ash content of 8.23 ± 0.11%, while AC2 recorded 7.03 ± 0.01%. The moisture contents of AC1 and AC2 were 7.61 ± 0.02% and 7.05 ± 0.04%, respectively, indicating that both samples were well dried and properly stored. The volatile matter contents were 15.04 ± 0.15% for AC1 and 14.87 ± 0.05% for AC2. , The fixed carbon contents were 69.12 ± 0.01% for AC1 and 71.05 ± 0.04% for AC2. These values indicate good-quality activated carbon, as fixed carbon content is typically expected to be ≥65% for effective adsorbents (Olayiwola *et al.*, 2015). (Olayiwola *et al.*, 2015).

**Table 1: Physicochemical properties of activated carbons (AC1 and AC2)**

Parameters	AC1	AC2
Ash Content(%)	8.23±0.11	7.03±0.01
Moisture Content(%)	7.61±0.02	7.05±0.04
Volatile Matter(%)	15.04±0.15	14.87±0.05
Fixed Carbon(%)	69.12±0.01	71.05±0.04
pH	7.02±0.11	7.07±0.06
Conductivity(µS/cm)	0.05±0.03	0.09±0.11
Bulk Density(g/cm <sup>3</sup> )	0.52±0.02	0.48±0.01
% Yield	30.05±0.04	36.6±0.13

**\*AC1 = Activated carbon prepared using H<sub>3</sub>PO<sub>4</sub> activation and AC2 =Activated carbon prepared using ZnCl<sub>2</sub> activation**

The pH values of AC1 and AC2 were 7.02 ± 0.11 and 7.07 ± 0.06, respectively. The pH of activated carbon is important to the adsorption of pollutants in solution, and for

most applications, the pH of activated carbon of 6.5-7.5 is accepted (Ahmedna *et al.*, 2000; Idris *et al.*, 2013). Activated carbon with adequate bulk density improves filtration



efficiency by forming a uniform filter cake on the filtration surface. The conductivity test is important because it shows the presence of leachable ash, which is considered impurity and undesirable (Khadija *et al.*, 2007). The  $0.05 \pm 0.03$  and  $0.09 \pm 0.11$   $\mu\text{S}/\text{cm}$  are the conductivities for the activated carbons, which indicate that the adsorbents contain less leachable ash. The activated carbons' bulk density was found to be  $0.52 \pm 0.02$  and  $0.48 \pm 0.01$   $\text{g}/\text{cm}^3$ , respectively. The activated carbons indicated a percentage yield of  $36.5 \pm 0.04$  for AC1 and  $40.5 \pm 0.13$  for AC2, respectively.

### 3.2 Characteristic Properties of Activated Carbon

#### 3.2.1 Brunauer-Emmett-Teller (BET)

The textural properties of the activated carbons, including surface area, pore volume, and pore diameter, are presented in Table 2. These parameters are critical in determining the adsorption performance of porous carbon materials. Carbonization temperature enhances thermal degradation and promotes the removal of volatile components from the precursor, thereby facilitating pore formation and development of a porous structure (Kumar and Jena, 2016).

As shown in Table 2, AC2 exhibited a higher BET surface area ( $976.48$   $\text{m}^2/\text{g}$ ) compared to AC1 ( $815.38$   $\text{m}^2/\text{g}$ ). This indicates that  $\text{ZnCl}_2$  activation was more

effective in enhancing surface development than  $\text{H}_3\text{PO}_4$  under the conditions employed. The superior performance of  $\text{ZnCl}_2$  may be attributed to its strong dehydrating and cross-linking effects, which promote aromatization and inhibit excessive tar formation during carbonization, thereby preserving the carbon framework and generating a more developed porous structure (Ho, 2022).

Similarly, the pore volume analysis in Table 2 shows that AC2 recorded a higher total pore volume ( $0.46$   $\text{cm}^3/\text{g}$ ) than AC1 ( $0.30$   $\text{cm}^3/\text{g}$ ). This increase is consistent across both micropore volume ( $0.29$   $\text{cm}^3/\text{g}$  for AC2 vs  $0.18$   $\text{cm}^3/\text{g}$  for AC1) and mesopore volume ( $0.17$   $\text{cm}^3/\text{g}$  for AC2 vs  $0.12$   $\text{cm}^3/\text{g}$  for AC1), indicating that  $\text{ZnCl}_2$  not only enhances overall porosity but also promotes the development of both micro- and mesoporous structures. The presence of a well-developed microporous network suggests improved adsorption capacity for small molecules, while mesopores facilitate diffusion and mass transport of larger adsorbate species into the internal structure of the carbon matrix (Yorgun and Yildiz, 2015). In contrast, AC1 exhibited a slightly larger average pore diameter ( $2.30$  nm) compared to AC2 ( $2.13$  nm), suggesting that phosphoric acid activation may favour the formation of relatively wider pores, although with lower overall pore volume and surface area. This difference indicates that  $\text{H}_3\text{PO}_4$  tends to promote pore widening, whereas  $\text{ZnCl}_2$  favours pore generation and densification of the porous network.

**Table 2: Surface area and pore size characterization of the activated carbons**

Parameters	AC1	AC2
BET Surface Area( $\text{m}^2/\text{g}$ )	815.38	976.48
Micropore volume( $\text{cm}^3/\text{g}$ )	0.18	0.29
Mesopore volume( $\text{cm}^3/\text{g}$ )	0.12	0.17
Total pore volume ( $\text{cm}^3/\text{g}$ )	0.30	0.46
Pore diameter (nm)	2.30	2.13



Overall, the results in Table 2 demonstrate that AC2 possesses superior textural properties compared to AC1 in terms of surface area and pore volume, making it more suitable for adsorption-based applications. The higher surface area and pore volume of AC2 imply enhanced adsorption capacity, improved accessibility of active sites, and better performance in environmental remediation.

### 3.2.2 Fourier Transform Infrared (FTIR) Analysis

FTIR spectroscopy was employed to identify the surface functional groups present in the prepared activated carbons, thereby providing insight into their surface chemistry, reactivity, and potential adsorption mechanisms, which are essential for industrial applications (González-García, 2018). The FTIR spectra of AC1 and AC2 are presented in Figs. 1 and 2, respectively.

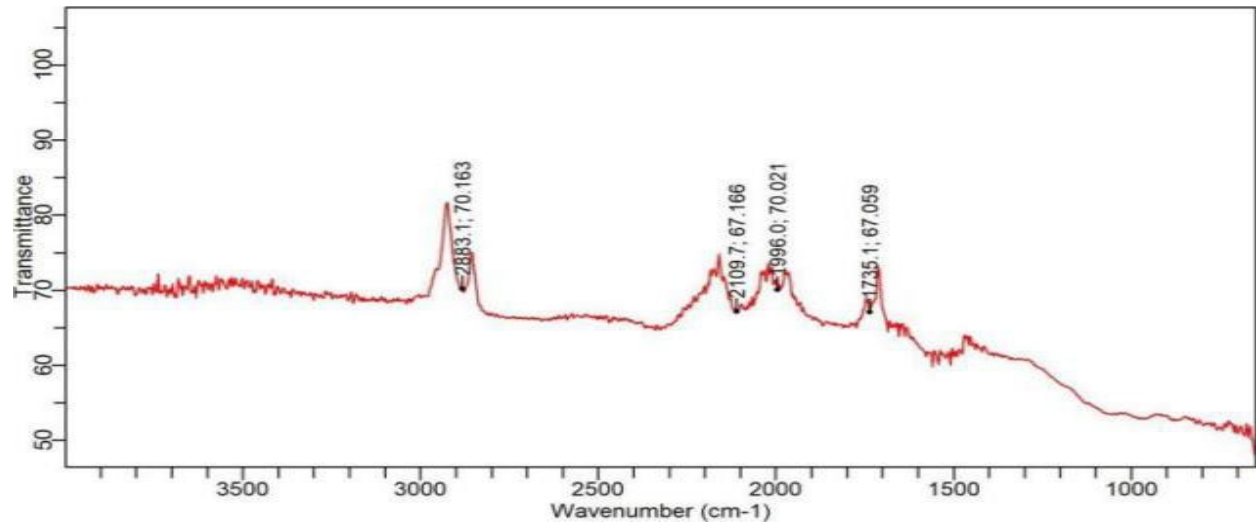


Fig. 1: FTIR spectral of AC1

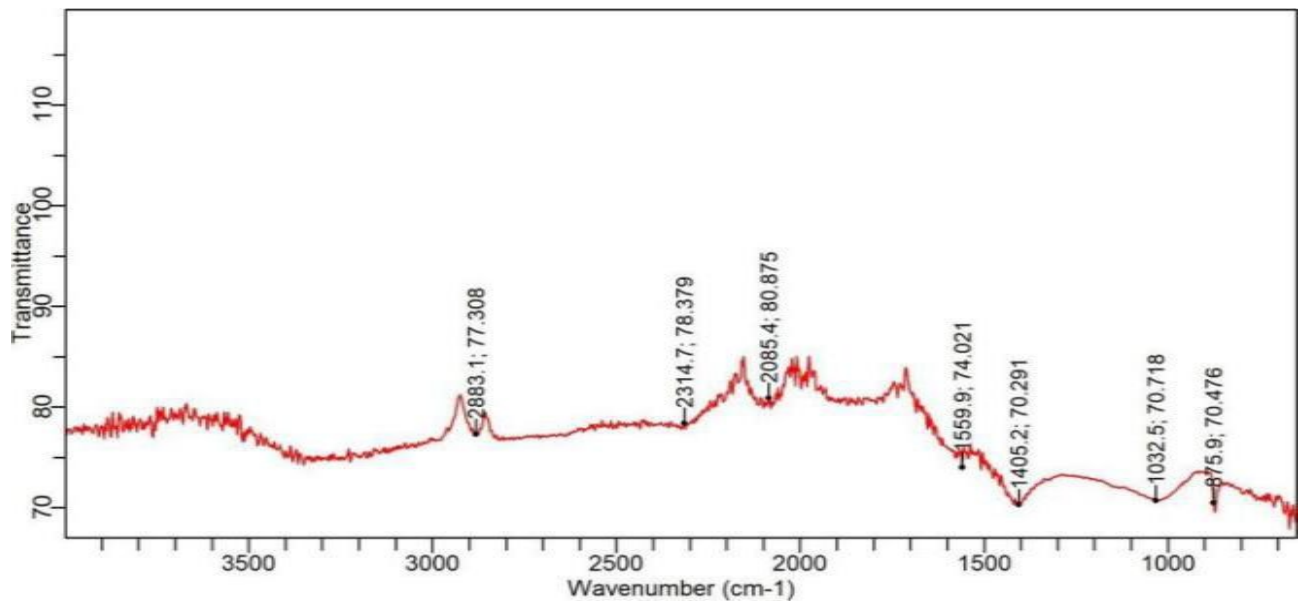


Fig. 2: FTIR spectral of AC2



As shown in Fig. 1 (AC1), several characteristic absorption bands were observed. The peak at  $1735.1\text{ cm}^{-1}$  is attributed to C=O stretching vibrations, indicating the presence of carbonyl or carboxylic functional groups, which are known to enhance adsorption of polar contaminants through hydrogen bonding and dipole–dipole interactions. The band at  $1996.0\text{ cm}^{-1}$  may be associated with conjugated C=C or cumulated double bond systems (C=C=C), suggesting the presence of unsaturated carbon structures within the activated carbon matrix.

Furthermore, the peaks at  $2109.7\text{ cm}^{-1}$  and  $2883.1\text{ cm}^{-1}$  are assigned to C≡C (alkyne stretching) and aliphatic C–H stretching vibrations, respectively. The presence of these functional groups indicates a partially aromatized carbon structure with residual aliphatic and unsaturated components, which contribute to diverse adsorption interactions.

In contrast, Fig. 2 (AC2) shows a slightly different surface functional group distribution. The band at  $875.9\text{ cm}^{-1}$  is associated with C=C bending vibrations, indicating aromatic ring structures on the carbon surface. The peak at  $1032.5\text{ cm}^{-1}$  corresponds to C–O stretching vibrations, suggesting the presence of oxygen-containing functional groups such as alcohols, phenols, or ethers, which enhance hydrophilicity and adsorption affinity for polar species. Additionally, the band at  $2883.1\text{ cm}^{-1}$ , common to both samples, is attributed to C–H stretching vibrations, indicating the persistence of aliphatic moieties in both activated carbons.

A comparative analysis of both spectra (Figs. 1 and 2) reveals that AC2 exhibits more pronounced oxygen-containing functional groups (C–O), while AC1 shows stronger signatures of carbonyl (C=O) and

unsaturated carbon species (C≡C and C=C=C). This difference is directly related to the activating agents used: ZnCl<sub>2</sub> activation tends to promote dehydration and incorporation of oxygenated surface functionalities, whereas H<sub>3</sub>PO<sub>4</sub> activation often leads to the development of more carbonyl-rich and unsaturated carbon frameworks.

The coexistence of oxygenated functional groups and aromatic structures in both samples indicates a chemically active surface capable of strong interactions with pollutants through mechanisms such as hydrogen bonding,  $\pi$ – $\pi$  interactions, and electrostatic attraction. However, the higher abundance of C–O functional groups in AC2 suggests improved surface polarity and enhanced adsorption potential for heavy metals and polar organic contaminants.

Overall, the FTIR results (Figs. 1 and 2) confirm that both activation methods successfully modified the surface chemistry of palm kernel shell-derived activated carbon, but ZnCl<sub>2</sub> activation (AC2) produced a more functionally diverse and potentially more reactive adsorbent. This implies that AC2 may exhibit superior performance in adsorption-based environmental remediation, particularly in wastewater treatment applications involving polar or ionic pollutants.

#### 4.0 Conclusion

Highly porous and surface area activated carbons were prepared from Palm Kernel shells using H<sub>3</sub>PO<sub>4</sub> and ZnCl<sub>2</sub> as activating agents. Physicochemical properties of activated carbons, namely ash content, were found to be  $8.23\pm 0.11$  for AC1 and  $7.03\pm 0.01$  for AC2; volatile matters of  $15.04\pm 0.15\%$  for AC1 and  $14.87\pm 0.05\%$  for AC2 and high fixed carbon of  $69.12\pm 0.01\%$  for AC1 and  $71.05\pm 0.04\%$  for AC2, respectively. The BET surface area of  $976.48\text{ m}^2/\text{g}$  recorded for AC2 was high compared to  $815.38\text{ m}^2/\text{g}$  indicated



for AC1. This could be attributed to the fact that  $ZnCl_2$  acts as a dehydrating agent, which allows more carbon to be kept fixed and alters the structure to make it more porous and well-developed (HO, 2022). AC1 spectral showed the peak occurrence at  $1735.1\text{ cm}^{-1}$  which may be attributed to the C = O stretching vibration and the presence of the absorption band at  $1996.0\text{ cm}^{-1}$  is responsible for the presence of C = C = C stretching vibration. Also for AC2 spectral, the presence of the peak at  $875.9\text{ cm}^{-1}$  indicates C = C stretching vibration, while the peak at  $1032.5\text{ cm}^{-1}$  reveals C-O stretching vibration.

### Acknowledgements

The authors are grateful to all the laboratory technologists, Department of Chemistry, Federal University of Technology Minna, Niger State, Nigeria, for their support during the research period.

### 5.0 References

- Abioye, A. M. & Ani, F. N.(2015). Recent Development In The Production Of Activated Carbon Electrodes From Agricultural Waste Biomass For Supercapacitors: A Review, *Renewable And Sustainable Energy Reviews*, 52, pp. 1282-1293.
- Ahmedna, M., Marshall, W. E, & Rao, R. M. (2000). Granular activated carbon from agricultural by-products: Preparation, properties and application in cane sugar refining. *Bulletin of Louisiana State University Agricultural Center*: 54, pp.1-57.
- Boadu, K. O., Joel, O. F., Essumang, D. K. & Evbuomwan, B. (2018). Comparative Studies of the Physicochemical Properties and Heavy Metals adsorption Capacity of Chemical Activated Carbon from Palm Kernel, Coconut and Groundnut Shells. *Journal of Applied Science Environmental Management*. 22, 1, pp. 1833–1839.
- Danish, M. & Ahmad, T. (2018). A Review On Utilization Of Wood Biomass As A Sustainable Precursor For Activated Carbon Production And Application, *Renewable And Sustainable Energy Reviews*, 87, pp. :1-21.
- Fan, M., Marshall, W., Dangaard, D. % Brown, C.(2005). Steam activation of chars produced from oat hulls. *Bioresource. Technology*. 93, pp. 103-107.
- González-García, P. (2018). Activated Carbon From Lignocellulosics Precursors: A Review Of The Synthesis Methods, Characterization Techniques And Applications, *Renewable And Sustainable Energy Reviews*, 82, pp. 393-1414.
- Ho, S. M. (2022). A Review of Chemical Activating Agent on the Properties of Activated Carbon. *International Journal of Chemistry and Research*. S1, 1, pp. 1-13.
- Idris, S., Yisa, J., Ndamitso, M. M. & Anyachukwu, C. C. (2013). Equilibrium and Adsorption Studies of Malachite Green onto Melon Seed Shell Activated Carbon. *International Journal of Modern Chemistry*, 4, 2, pp. 90-103.
- Jalalah, M., Rudra, S., Aljafari, B., Irfan, M., Almasabi, S. S., Alsuwian, T., Patil, A. A., Nayak, A. K & Harraz F. A. (2021). Novel Porous Heteroatom-Doped Biomass Activated Carbon Nanoflakes For Efficient Solid-State Symmetric Supercapacitor Devices, *Journal Of The Taiwan Institute Of Chemical Engineers*, 132, pp. 215-223.
- Karthikeyan, S., Jo, W. K., Dhanalakshmi, R., Isaacs, M. A., Wilson, K., Sekaran, G. & Lee, A. F. (2018). A Porous Activated Carbon Supported Pt Catalyst For The Oxidative Degradation Of Poly (Naphthalene formaldehyde) Sulfonate,



- Journal of the Taiwan Institute of Chemical Engineer*, 93, pp, 289-297.
- Khadija, Q, Inamullah, B., Rafique, K. & Abdul, K. A. (2007). Physical and chemical analysis of activated carbon prepared from sugarcane bagasse and use for sugar. *World Acad. Sci. Eng. Tech.*, 34, pp. 194-198.
- Kumar, A. & Jena, H. M. (2016). Preparation and characterization of high surface area activated carbon from Fox nut (*Euryale ferox*) shell by chemical activation with  $H_3PO_4$ . *Results in Physics*, 6, pp. 651–658
- Olayiwola, A. O., Adebisi, S. S., Alapinni, T. J. & Amuda, OS (2015). Preparation and Characterization of Activated Carbon Originated from Yam Set and Yam Peel. *Conference proceedings International Conference for Sustainable Development (ICSD) in 21st Century in Africa*, Organized by The Post Graduate School, Ladoke Akintola University of Technology Ogbomoso, Nigeria. 251-261.
- Onawumi, O. O.E., Sangoremi, A. A. & Bello, O.S. (2021). Preparation and Characterisation of Activated Carbon from Groundnut and Egg Shells as Viable Precursors for Adsorption. *Journal of Applied Science Environmental Management*. 25, 9, pp. 1707-1713
- Okiemen, F. E. Ojoku, F. I., Okiemen, C. D. & Wuana, R. A. (2024). Preparation and evaluation of activated carbon from rice husk and rubber seed shell. *Chem. J.* 23, pp. 191-196.
- Rahman, I. A., Said, B., Shadier, S. O. & Syarizal, E. S.(2005). Adsorption characteristic of malachite green an activated carbon derived from rice husk produced by chemical thermal process. *Bioresource Technology*. 95, pp. 1578-1583.
- Sánchez-Cantú, M., Janeiro-Coronel, V. J., Galicia-Aguilar, J. A. and Santamaría-Juárez, J. D. (2018). Effect of the activation temperature on activated carbon production from castor cake and its evaluation as dye adsorbent, *International Journal of Environmental Science and Technology*, 15, 7, pp. 1521-1530.
- Tongpoothorn, W., Sriuttha, M., Homchan, P., Chanthai, S. & Ruangviriyachai, C (2011). Preparation Of Activated Carbon Derived From *Jatropha Curcas* Fruit Shell By Simple Thermo-Chemical Activation And Characterization Of Their Physico-Chemical Properties, *Chemical Engineering Research And Design*, 89, 3, pp. 335-340.
- Wang, G., Qian, B., Dong, Q., Yang, J., Zhao, Z. & Qiu, J. (2013). Highly Mesoporous Activated Carbon Electrode For Capacitive Deionization, *Separation and Purification Technology*, 103, pp. 216-221.
- Xin-Hui, D., Srinivasakannan, C., Jin-Hui, P., Li-Bo, Z. and Zheng-Yong, Z. (2011). Preparation Of Activated Carbon From *Jatropha* Hull With Microwave Heating: Optimization Using Response Surface Methodology, *Fuel Processing Technology*, 92, 3, pp. 394-400.
- Yorgun, S. & Yıldız, D. (2015). Preparation And Characterization Of Activated Carbons From *Paulownia* Wood By Chemical Activation With  $H_3PO_4$ , *Journal of the Taiwan Institute of Chemical Engineers*, 53 :122-131.
- Yulu, D., Walawender, W. & Fan, L.(2001). Activated Carbons Prepared from Phosphoric Acid Activation of Grain Sorghum. *Bioresource Technology*, 81, 1, pp. 45-52.
- Zubrik, A., Matik, M., Hredzák, S., Lovás, M., Danková, Z., Kováčová, M. & Briančin, J.(2017). Preparation Of Chemically Activated Carbon From Waste Biomass



By Single-Stage And Two-Stage  
Pyrolysis, *Journal Of Cleaner  
Production*, 143, pp. 643-653.

**Declaration**

**Consent for publication**

Not Applicable

**Availability of data and materials**

The publisher has the right to make the data  
public

**Conflict of Interest**

The authors declared no conflict of interest

**Ethical Considerations**

Not applicable

**Competing interest**

The authors report no conflict or competing  
interest

**Funding**

The author declared no source of funding

**Authors' Contributions**

Suleiman Idris conceptualized the study, supervised the research, and reviewed the manuscript. Yunusa Muhammad Boyi contributed to methodology design and data analysis. Wasiu Jamiu carried out laboratory experiments and data collection. Nura Kontagora assisted in characterization and interpretation of results. Precious Adepeju Job participated in sample preparation and manuscript drafting. All authors read and approved the final manuscript.

